

## SYNTHESIS AND CHARACTERIZATION OF MAGNETIC-HYDROXYAPATITE COMPOSITE USING ONE-SPOT COPRECIPITATION METHOD

Mujamilah<sup>1</sup>, Ahmad Furqon Syidik<sup>2</sup>, Grace Tj. Sulungbudi<sup>1</sup>,  
Wildan Z. Lubis<sup>1</sup> and Aloma Karo Karo<sup>1</sup>

<sup>1</sup>Centre for Science and Technology of Advanced Material (PSTBM) - BATAN  
Kawasan Puspiptek, Serpong 15314, Tangerang Selatan

<sup>2</sup>Department of Chemistry, Bogor Agricultural University

Jl. Dramaga, Bogor 16003

E-mail: [ian@batan.go.id](mailto:ian@batan.go.id)

Received: 23 September 2016    Revised: 15 December 2016    Accepted: 28 December 2016

### ABSTRACT

**SYNTHESIS AND CHARACTERIZATION OF MAGNETIC-HYDROXYAPATITE COMPOSITE USING ONE SPOT COPRECIPITATION METHOD.** Nanocomposite of magnetic-hydroxyapatite (MHAP) has the potential to be developed as a biocompatible-biodegradable material for bone cancer diagnosis and therapy. In this study, such composite materials have been successfully synthesized by one-spot coprecipitation method and ultrasonic dispersion. The mass ratio between magnetic and hydroxyapatite fraction were varied to 30:70 (K30), 40:60 (K40) and 50:50 (K50). X-Ray Diffractometer, Transmission Electron Microscope, Fourier Transform-Infrared Spectrometer and Vibrating Sample Magnetometer were used for characterizing the properties of MHAP composite. X-Ray Diffraction pattern reveals the presence of magnetic and HAP phases, confirm the establishment of MHAP composite system. TEM image and FT-IR spectra shows the spherical morphology of magnetic nanoparticles with a size of ~ 10 nm entrapped within HAP nanorod structure without any chemical bonding between the two phase. With such physical composite mechanism and higher energy induce by ultrasonic dispersion process, magnetic fraction of even 50% mass fraction could still be loaded into HAP matrix and provide maximum magnetisation value of 34.6 emu/g. This magnetization value is higher than the result of another study of MHAP synthesis, giving better prospect for bone cancer diagnosis and therapy.

**Keywords:** Composite, Magnetite, Maghemite, Hydroxyapatite, One-spot coprecipitation

### ABSTRAK

**SINTESIS KOMPOSIT MAGNETIK-HIDROKSIAPATIT DENGAN METODE KO-PRESIPITASI SATU TAHAP DAN KARAKTERISASINYA.** Nanokomposit magnetik-hidroksiapatit (MHAP) berpotensi dikembangkan sebagai bahan *biocompatible-biodegradable* untuk diagnosis dan terapi kanker tulang. Dalam studi ini, bahan komposit tersebut telah disintesis dengan metode ko-presipitasi satu tahap diikuti dengan proses dispersi ultrasonik. Perbandingan fraksi massa antara bahan magnetik dan hidroksiapatit divariasikan dengan komposisi 30:70 (K30), 40:60 (K40) dan 50:50 (K50). *X-Ray Diffractometer (XRD)*, *Transmission Electron Microscope (TEM)*, *Fourier Transform-InfraRed (FT-IR) Spectrometer* dan *Vibrating Sample Magnetometer (VSM)* digunakan untuk mengkarakterisasi sifat-sifat komposit MHAP. Pola difraksi sinar-X menunjukkan hadirnya fase magnetik dan HAP, mengkonfirmasi terbentuknya sistem komposit MHAP. Gambar *TEM* dan spektra *FT-IR* menunjukkan adanya nanopartikel berbentuk bulat dengan ukuran ~ 10 nm yang terperangkap di dalam struktur nanorod HAP tanpa adanya ikatan kimia di antara kedua fase tersebut. Dengan mekanisme komposit fisis tersebut serta proses dispersi ultrasonik, 50% fraksi massa magnetik masih dapat dimuatkan ke dalam matriks HAP dan menghasilkan nilai magnetisasi komposit hingga 34,6 emu/g. Nilai magnetisasi ini lebih tinggi dari hasil studi sintesis MHAP lainnya, memberi prospek yang lebih baik untuk diagnosis dan terapi kanker tulang.

**Kata kunci:** Komposit, Magnetit, Maghemit, Hidroksiapatit, *One-spot coprecipitation*

## INTRODUCTION

Hydroxyapatite (HAP) is widely known as one of material for bone regeneration. Having a chemical composition of  $\text{Ca}_{10}(\text{PO}_4)_6(\text{OH})_2$ , which is similar to the composition of human bones, synthetic HAP has been used in healing or recovery of broken bones [1]. Recently, considerable research were carried out on combining HAP with magnetic nanoparticle [2-5]. Magnetic nanoparticle has been developed to be applied in some biomedical field due to its magnetic properties that can support diagnostic as well as therapeutic process. Usually the surface of nanoparticles must be modified first with organic or inorganic coating to get biocompatible system fit for such application [6]. Composite between HAP and magnetic nanoparticle (MHAP) is expected to give biocompatible ceramic magnetic materials which would be applied as an MRI contrast agent for diagnostic application as well as hyperthermia agent for therapy of bone cancer [4-5,7]. There are two general routes for synthesizing this composite, two-steps and one-step method. Two-steps method is carried out in which magnetic nanoparticle and HAP separately synthesized before mixing them to form composite. This synthesis route is performed using microemulsion [2], hydrothermal [4], mechanochemical process [5], and spray drying or spray pyrolysis technique [7,8]. All these processes usually result in the formation of hundreds size of composite particles having low magnetization value due to high fraction of HAP within the composite. Other route employing one-step precipitation process is accomplished by mixing all the precursor of magnetite and HAP at once followed by addition of strong base solution and some sequential treatment to establish the formation of MHAP precipitate [3]. This process, indeed, give higher magnetic saturation but still too low comparing to theoretical calculation due to low magnetization value of magnetic nanoparticle being precipitate within HAP matrix.

In this article, we report the synthesis of an MHAP nano-composite which has higher magnetization value. The synthesis was conducted in one-spot co-precipitation of magnetic and HAP fraction with different mass ratio followed by ultrasonic irradiation. Chemical and physical characteristics of the composite were thoroughly evaluated for understanding the mechanism inducing composite characteristics.

## EXPERIMENTAL METHOD

### Materials and Equipment

All chemicals are used as received without special treatment.  $\text{FeCl}_3 \cdot 6\text{H}_2\text{O}$ ,  $\text{FeCl}_2 \cdot 4\text{H}_2\text{O}$ ,  $\text{Ca}(\text{NO}_3)_2 \cdot 4\text{H}_2\text{O}$ ,  $(\text{NH}_4)_2\text{HPO}_4$ , and glacial acetic acid was obtained from Merck (Germany). Another materials used are  $\text{NH}_4\text{OH}$ , nitrogen gas (UHP),  $\text{NaOH}$  and Deionized

Water. The equipment for mixing and homogenizing are ultrasonic probe "Sonics" (20 kHz, 40 watts) and IKA Eurostar Mixer. Other equipment used is glassware, stirrer and ovens.

### MHAP Composite Preparation

MHAP composite was synthesized by following the method of Nguyen VC et al [3] with slight modification using ultrasonic irradiation instead of mechanical stirring. The samples were prepared with magnetic to HAP mass ratio of 30:70, 40:60 and 50:50 which denoted as K30, K40 and K50 samples respectively.  $\text{FeCl}_3 \cdot 6\text{H}_2\text{O}$  and  $\text{FeCl}_2 \cdot 4\text{H}_2\text{O}$  were dissolved in deionized water which has been aerated with nitrogen gas. Some volume of 25%  $\text{NH}_4\text{OH}$  solution was added to these salts solution and dispersed with ultrasonic probe for 5 minutes.  $\text{Ca}(\text{NO}_3)_2 \cdot 4\text{H}_2\text{O}$  and  $(\text{NH}_4)_2\text{HPO}_4$  were dissolved in deionized water and added slowly to the previous solution. The pH value of the mixture was adjusted to 11 and continued with ultrasonic irradiating process for another 5 minutes. The solution was then heated at 90 °C for 2 hours while stirring using a mechanical mixer. The black solution was allowed to cool to room temperature, and then allowed to further precipitate for 24 hours without stirring. The precipitate was then separated using permanent magnet and washed with deionized water until it reached a neutral pH. After drying in an oven at a temperature of 90 °C for 1 hour, the precipitate was pulverized using a mortar. MHAP fine powder obtained were then characterized to determine its properties.

### Characterization

Characterizations were carried out to determine the phases, magnetic properties, chemical bonding formed between the components of MHAP composites and their morphology. The phases were analyzed from diffraction pattern collected using PANalytical X-Ray Diffractometer with Cu radiation source ( $\lambda = 0.154056$  nm) in the range of diffraction angles,  $2\theta$  10° - 90°. Detail phase and structure analysis were carried out using RIETAN 2000 program [9]. Magnetic properties were analyzed from the hysteresis curve measured using Vibrating Sample Magnetometer (VSM) OXFORD 1.2H. Measurements were performed at room temperature with an external magnetic field up to 1 Tesla. Analysis of chemical interactions between the components of the composite was performed using Bruker FTIR spectrophotometer Tensor 27 equipped with ATR system. These three facilities are installed at Centre for Science and Technology of Advanced Material (PSTBM), BATAN. Morphology of MHAP composite was observed and analyzed using Transmission Electron Microscope (TEM) JEOL JEM 1400 at Chemistry Departement of Universitas Gadjah Mada.

## RESULT AND DISCUSSION

### XRD Analysis

MHAP sample diffraction pattern in Figure 1, shows the formation of  $\text{Fe}_3\text{O}_4$  (magnetite) phase, identified from the presence of peaks at an angle of  $30.30^\circ$ ,  $35.70^\circ$ ,  $43.40^\circ$ ,  $57.40^\circ$ , and  $63.10^\circ$ , fit with the data on crystallography database (JCPDS ICDD 19-629) for  $\text{Fe}_3\text{O}_4$  [10].

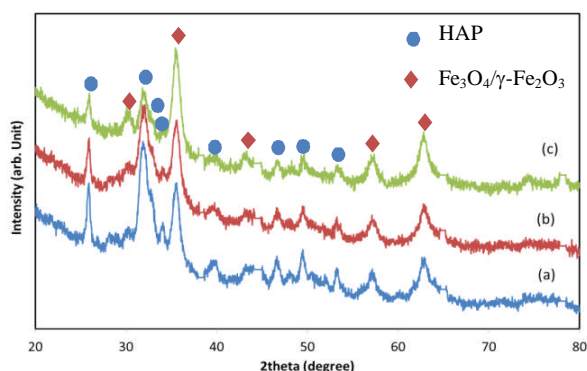
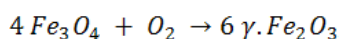


**Figure 1.** X-ray diffraction pattern of magnetic-hydroxyapatite composites at different composition: (a). K30; (b). K40 and (c). K50.

The peaks are broadened which indicates the formation of nanocrystalline structure. These peaks could also be identified as the peak of maghemite,  $\gamma\text{-Fe}_2\text{O}_3$  (JCPDS-ICDD 39-1346) [10] for these two phases are isomorphous. This second phase is very likely to occur because the magnetite can be oxidized to maghemite on MHAP synthesis process, especially during the heating process, following chemical reaction of:



Hydroxyapatite (HAP) phase is identified by the appearance of HAP typical peaks at an angle of  $25.95^\circ$ ,  $31.71^\circ$ ,  $32.19^\circ$ ,  $32.90^\circ$ ,  $39.47^\circ$ ,  $46.70^\circ$ ,  $49.50^\circ$  and  $53.25^\circ$  fit with the data on JCPDS (9-432). Peaks of HAP showed normal peak to peak ratio or did not show any preferred orientation, indicate the formation of HAP of granular or short-rod structure [11]. Figure 2 shows that HAP peaks also broadened and there is no clear splitting of (211), (112) and (300) peaks in the range of  $31^\circ$  to  $33^\circ$  diffraction angle which indicates a low degree of HAP crystallinity. This low crystallinity is analyzed due to the HAP precipitation is accomplish only by strong base solution environment [12], followed by low temperature heating at  $90^\circ\text{C}$ , simultaneously with the precipitation of magnetic nanoparticles. Increasing magnetic fraction results in lowering intensity and more broaden HAP peaks, hence more amorphous HAP. This condition is related once again with the fact of only strong base induce precipitation. Higher magnetic fraction will consume more base solution and leaving only a small

volume of base for HAP precipitation and consequently will lower HAP degree of crystallinity.

For magnetic phase (see Figure 2), more detail observation on (311) principal peak of magnetite phase at  $35.70^\circ$ , it can be seen that no significant change of peak broadening with increasing magnetic fraction, ensuring nearly the same crystallite size of magnetite nanoparticle for all composition. The crystallite size is about 5 nm, estimated using Debye-Scherrer equation.

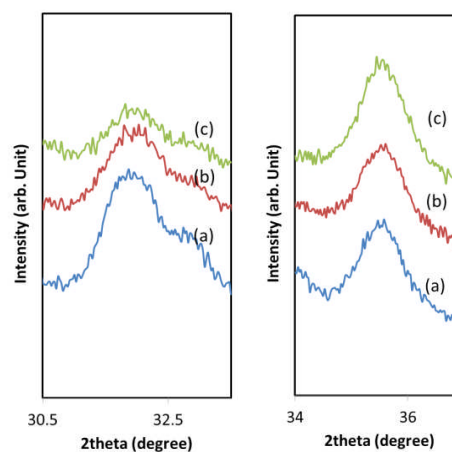


**Figure 2.** Detail diffraction pattern of HAP ( $30.5^\circ - 33.5^\circ$ ) and  $\text{Fe}_3\text{O}_4/\gamma\text{-Fe}_2\text{O}_3$  ( $34^\circ - 37^\circ$ ) principal peaks for (a). K30; (b). K40 and (c). K50 samples.

These magnetic and HAP phases are bound to each other forming a composite of MHAP. This conclusion comes from the fact that the sample was obtained as a result of washing and separation process using permanent magnets.

If these phases are not bound to each other, then HAP will not be attracted by magnet and will be left at the solution during the washing step, leaving only magnetic phase powder as a synthesis product.

Further analysis on the patterns were carried out using Rietveld analysis method implemented on RIETAN2000 program [9] and HAP base structure parameter from article written by Petr Ptacek [13]. Figure 3 shows refined pattern of each composite sample, assuming the existence of three phases of  $\text{Fe}_3\text{O}_4$ ,  $\gamma\text{-Fe}_2\text{O}_3$  and HAP. The refined patterns were well fitted with the observation patterns and give the reliability factor,  $R_{wp} \sim 2$  and goodness of fit,  $S \sim 1.5$ . Detail composition and refined parameter results are presented in Table 1.

There is slight changing of lattice parameter of  $\text{Fe}_3\text{O}_4/\gamma\text{-Fe}_2\text{O}_3$  to smaller value compared to their initial lattice parameter of  $\sim 8.4 \text{ \AA}$  while HAP lattice parameter show no changing with varying composition. It could be analyzed that magnetic nanoparticles growth were slightly inhibited by surrounding HAP phase and result in suppressing magnetic lattice. Refined composition tend to deviate from their initial value give non-linear relationships with increasing magnetic fraction analyzed due to unhomogenized mixing process.

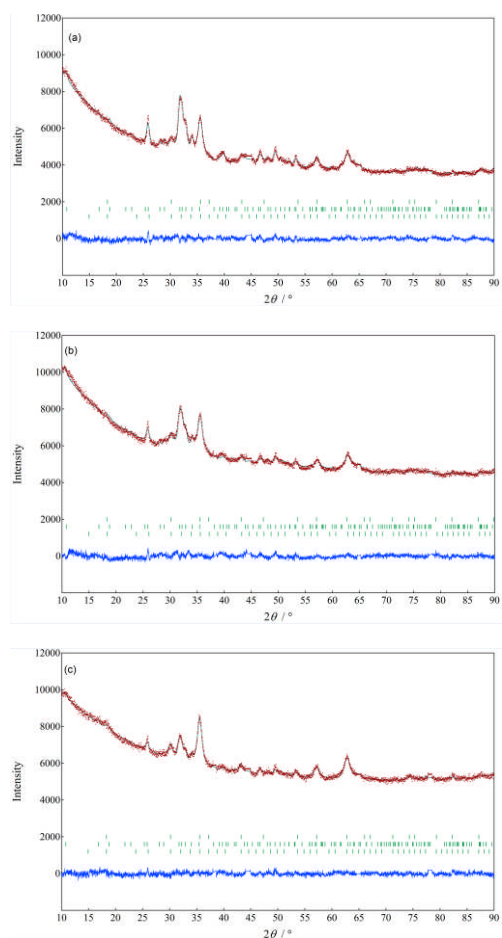


Figure 3. Refined pattern of each composite sample.

Table 1. Rietveld refinement result of the MHAP samples of different compositions (calculate using space group of P63/M for hydroxyapatite [13], Fd3m for Fe<sub>3</sub>O<sub>4</sub> and P4132 for -Fe<sub>2</sub>O<sub>3</sub> [10])

Parameters	K30	K40	K50
R <sub>wp</sub> (Reliability factor)	2.08	1.88	1.58
S (goodness of fit)	1.4456	1.4307	1.2505
Compositions (wt%)			
- Fe <sub>3</sub> O <sub>4</sub>	21.81	22.69	35.32
- γ-Fe <sub>2</sub> O <sub>3</sub>	6.58	12.18	17.98
- Hydroxyapatite	71.61	65.13	46.70
Lattice parameter (Å)			
Fe <sub>3</sub> O <sub>4</sub>			
- a = b = c	8.36388	8.37579	8.36000
γ-Fe <sub>2</sub> O <sub>3</sub>			
- a = b = c	8.36172	8.35565	8.36050
Hydroxyapatite			
- a = b	9.42472	9.41795	9.41955
- c	6.87578	6.87147	6.87755

Sample of K40 shows lower magnetic fraction with high maghemite fraction which is unfavourable for high magnetic properties establishment.

### TEM imaging and Particle Size Analysis

Morphology of K50 composite observed by TEM shown in Figure 4 confirm analyses result of X-ray diffraction pattern. Figure 4(a) displays the morphology

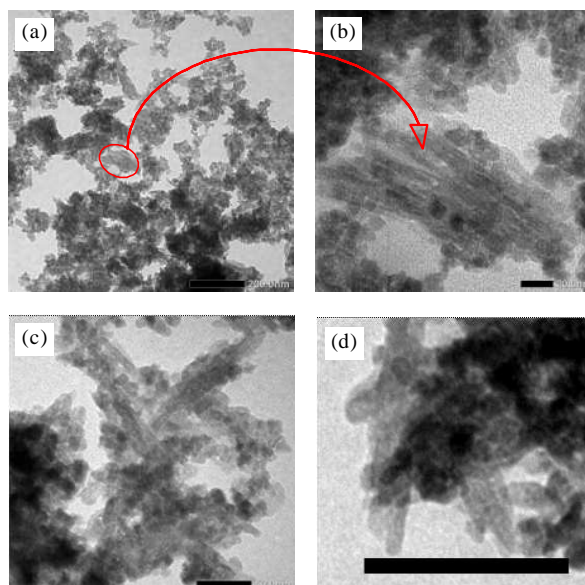


Figure 4. TEM image of K50 MHAP powder samples at different position and magnification (a). 1 scale = 200 nm; (b). 1 scale = 20 nm; (c). 1 scale = 50 nm; and (d). 1 scale 100 nm

of irregular shape composite having ~ 100 nm - 200 nm in size. More detail picture in Figure 4(b) shows the spherical morphology of magnetic nanoparticles (dark image) with a size of ~ 10 nm trapped within HAP needle like structure (gray image) and surrounding by the short rod of HAP structure (Figure 4(c) and 4(d)). This morphological picture support the synergetic growth mechanisms between magnetic nanoparticle and HAP nanorod structure, which are bound to one another forming nanocomposite system. This result is in agreement with other study of MHAP structures using energy filter imaging and electron tomography which showed that HAP nanoparticles tend to have a needle structure for the one interact directly with the surface of magnetic nanoparticle, while the surrounding HAP is more likely to form a rod structure [14].

The images also showed the more separate nanoparticles dispersed within HAP matrix, which is analyzed due to higher energy induce by ultrasonic process compared to the mechanical mixing.

This high energy and more monodisperse magnetic nanoparticle is assumed being responsible for higher fraction of magnetic nanoparticle as high as 50% that could be incorporated within HAP matrix. Other experiment using hydrothermal process stated that mass fraction of only 30% could maximally be entrapped [4].

### FT-IR Spectrum Analysis

Chemical bond presence in MHAP samples are analysed from their infrared spectrum as shown in Figure 5 measured using ATR technique. In MHAP spectrum there are absorption bands at 1452, 1410, which characterize the carbonate functional group. An

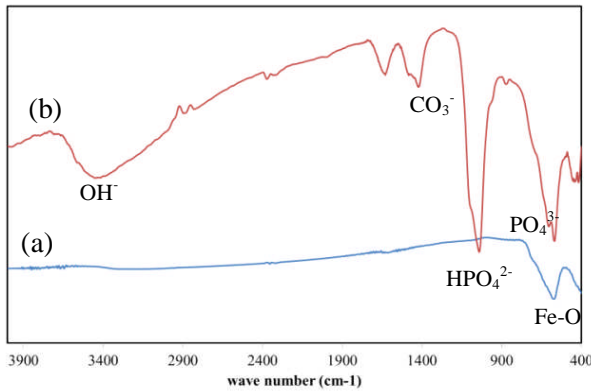


Figure 5. Infra red spectra of magnetite nanoparticle (a) and K50 composite (b).

absorption band at  $3525\text{ cm}^{-1}$  is produced by hydroxyl functional groups on MHAP and wave numbers  $1033$ ,  $572$ , and  $571\text{ cm}^{-1}$  in accordance with the functional groups on the HAP  $\text{PO}_4^{3-}$  [15]. Absorption band typical for Fe-O bond also appears at wave number  $570\text{ cm}^{-1}$ . The existence of this typical band of HAP and magnetite at MHAP spectra, revealed the formation of composite of magnetite-HAP. However, there is no chemical bond between magnetite and HAP phase, which assuring the more physical interaction between the phases.

### Magnetic Properties Analysis

The most important properties of these composites are their magnetic properties. These properties will be related to the ability of the composite to become an agents of hyperthermia therapy as well as an MRI contrast agent. Figure 6 displays magnetic hysteresis curve of MHAP composites measured at room temperature with a maximum external magnetic field of 1 Tesla. In general, MHAP samples show superparamagnetic properties, which usually obtained for  $\text{Fe}_3\text{O}_4$  nanoparticle with crystallite size below  $20\text{ nm}$  [16].

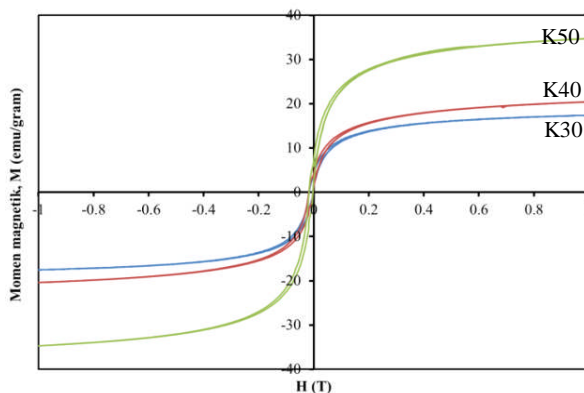


Figure 6. Magnetic hysteresis curve of MHAP composite for different composition

The saturation magnetization,  $M_s$  is the maximum value of magnetization that can be achieved when all

the magnetic moments aligned in one specific direction and will have the value of  $92\text{ emu/gram}$  for bulk and pure  $\text{Fe}_3\text{O}_4$  and  $76\text{ emu/gram}$  for  $\gamma\text{-Fe}_2\text{O}_3$  [17]. For MHAP K50, with real mass composition of  $53.3\%$  for magnetic fraction as discussed in (3.1) section, theoretically the  $M_s$  value should be in the range of  $(40.5 - 49.04)\text{ emu/gram}$ . However, the measurement result give only  $34.6\text{ emu/gram}$ . Referring to the discussion of phase and morphology above, this decrease could be explain due to the existence of two-phase mixture of  $\text{Fe}_3\text{O}_4$  and  $\gamma\text{-Fe}_2\text{O}_3$  phase and low degree of crystallinity of magnetic nanoparticle produce in this process. This fact also could be used to explain non-linear behaviour of magnetization for K40 sample as displayed in Figure 6.

The presence of HAP phase between the magnetic nano powders could also reduce magnetic interaction between iron oxide. When the magnetic nanoparticles bound firmly in the HAP rod system, it will reduce the freedom of magnetic nanoparticles to rotate and respond to any external magnetic field given to reach saturation value [18].

This K50 MHAP  $M_s$  values are still higher than the results of the same process but using mechanical stirrer [3], which only reach  $\sim 40\text{ emu/gram}$  for pure magnetic powder and would provide much lower magnetic value for MHAP. It can be assumed that ultrasonic irradiation used in this work provide faster precipitation of  $\text{Fe}_3\text{O}_4$  nanoparticles and inhibit further oxidation to  $\gamma\text{-Fe}_2\text{O}_3$ . Consequently, this will result, not only magnetic nanoparticles with smaller size and homogeneous, but also enhancement of magnetic phase formation. However, other research result show that too high ultrasonic frequency and power ( $35\text{ kHz}$ ,  $320\text{ W}$ ) will significantly decrease the magnetization to the value of only  $7.40\text{ emu/gram}$  which is analyzed due to the magnetic domain of the particle hindered by molecular binding with HAP [18]. Similarly, spray pyrolysis process, producing only a composite MHAP with a value of magnetization of  $11.8\text{ emu/gram}$  for  $36.4\%$  magnetic mass fraction [7] or about  $35\text{ emu/gram}$  of pure magnetite sample. Even for higher ratio between magnetite and HAP of  $3.2$ , the only maximum of  $30\text{ emu/gram}$  could be obtained by other spray pyrolysis process [8].

### CONCLUSION

High magnetization nanocomposite of magnetic-hydroxyapatite (MHAP) has been successfully synthesized by one-spot co-precipitation method and ultrasonic dispersion.  $\text{Fe}_3\text{O}_4/\gamma\text{-Fe}_2\text{O}_3$  magnetic nanoparticles with a size of  $\sim 10\text{ nm}$  entrapped within HAP nanorod structure without any chemical bonding between the two phases. With such physical composite mechanism and higher energy induce by ultrasonic dispersion process, magnetic fraction of even  $50\%$  mass fraction could still be loaded into HAP matrix and provide maximum magnetization value of  $34.6\text{ emu/gram}$ . It can

be concluded that MHAP produced in this study has a magnetization value higher than the synthesis of other similar studies and will have a prospect to produce better contrast in MRI image and desired heat for hyperthermia therapy.

## ACKNOWLEDGEMENTS

This work was supported by the DIPA of PSTBM-BATAN at fiscal year of 2015. The authors would like to thank PSTBM-BATAN management for providing this fund.

## REFERENCES

- [1]. M. A. Velasco, C. A. Narváez-Tovar, and D. A. Garzón-Alvarado. "Design, Materials, and Mechanobiology of Biodegradable Scaffolds for Bone Tissue Engineering." *Biomed Res. Int.*, vol. 2015, pp. 1-21, 2015.
- [2]. F. Foroughi, S. A. Hassanzadeh-Tabrizi, and J. Amighian. "Microemulsion Synthesis and Magnetic Properties of Hydroxyapatite-encapsulated nano  $\text{CoFe}_2\text{O}_4$ ." *J. Magn. Magn. Mater.*, vol. 382, pp. 182-187, 2015.
- [3]. V. C. Nguyen and Q. H. Pho. "Preparation of Chitosan Coated Magnetic Hydroxyapatite Nanoparticles and Application for Adsorption of Reactive blue 19 and  $\text{Ni}^{2+}$  ions." *Sci. World J.*, vol. 2014, pp. 1-9, 2014.
- [4]. S. Murakami, T. Hosono, B. Jeyadevan, M. Kamitakahara, and K. Ioku. "Hydrothermal Synthesis of Magnetite/Hydroxyapatite Composite Material for Hyperthermia Therapy for Bone Cancer." *J. Ceram. Soc. Japan*, vol. 116, no. 9, pp. 950-954, 2008.
- [5]. T. Iwasaki, R. Nakatsuka, K. Murase, H. Takata, H. Nakamura, and S. Watano. "Simple and Rapid Synthesis of Magnetite/Hydroxyapatite Composites for Hyperthermia Treatments Via A Mechano Chemical Route." *Int. J. Mol. Sci.*, vol. 14, no. 5, pp. 9365-9378, 2013.
- [6]. W. Wu, Z. Wu, T. Yu, and C. Jiang. "Recent Progress on Magnetic Iron Oxide Nanoparticles : Synthesis, Surface Functional Strategies and Biomedical Applications," *Sci. Technol. Adv. Mater.*, vol. 16, no. 2, pp. 1-43, 2015.
- [7]. A. Inukai et al. "Synthesis and Hyperthermia Property of Hydroxyapatite Ferrite Hybrid Particles by Ultrasonic Spray Pyrolysis." *J. Magn. Magn. Mater.*, vol. 323, no. 7, pp. 965-969, 2011.
- [8]. N. Wakiya, M. Yamasaki, T. Adachi, A. Inukai, and N. Sakamoto. "Preparation of Hydroxyapatite-Ferrite Composite Particles by Ultrasonic Spray Pyrolysis." *Mater. Sci. Eng. B*, vol. 173, no. 1-3, pp. 195-198, 2010.
- [9]. F. Izumi and T. Ikeda. "A Rietveld-Analysis Programm RIETAN-98 and Its Applications to Zeolites." *Mater. Sci. Forum*, vol. 321-324, pp. 198-205, 2000.
- [10]. Z. Danková and V. Zelenak. "Influence of Heat Treatment on Phase Transformation of Clay-Iron oxide composite." *J. Alloys Compd.*, vol. 511, pp. 63-69, 2012.
- [11]. M. Manoj, R. Subbiah, D. Mangalaraj, N. Ponpandian, C. Viswanathan, and K. Park. "Influence of Growth Parameters on The Formation of Hydroxyapatite (HAp) Nanostructures and Their Cell Viability Studies." *Nanobiomedicine*, vol. 2, no. 2, pp. 1-11, 2015.
- [12]. M. Wojasiński, E. Duszyńska, and T. Ciach. "Lecithin-Based Wet Chemical Precipitation of Hydroxyapatite Nanoparticles." *Colloid Polym. Sci.*, vol. 293, no. 5, pp. 1561-1568, 2015.
- [13]. P. Ptacek. "Introduction to Apatites." in *Apatites and their Synthetic Analogues-Synthesis, Structure, Properties and Applications*, INTECH, pp. 1-59, 2016.
- [14]. M. Okuda et al. "Structural Analysis of Hydroxyapatite Coating on Magnetite Nanoparticles Using Energy Filter Imaging and Electron Tomography." *J. Electron Microsc.* (Tokyo), vol. 59, no. 2, pp. 173-179, 2010.
- [15]. F. Heidari, M. E. Bahrololoom, D. Vashae, and L. Tayebi. "In Situ Preparation of Iron Oxide Nanoparticles in Natural Hydroxyapatite/Chitosan Matrix for Bone Tissue Engineering Application." *Ceram. Int.*, vol. 41, pp. 3094-3100, 2015.
- [16]. M. Nakaya, R. Nishida, and A. Muramatsu. "Size Control of Magnetite Nanoparticles in Excess Ligands as a Function of Reaction Temperature and Time." *Molecules*, vol. 19, no. 8, pp. 11395-11403, 2014.
- [17]. R. A. Ortega and T. D. Giorgio. "A Mathematical model of Superparamagnetic Iron Oxide Nanoparticle Magnetic Behavior to Guide The Design of Novel Nanomaterials." *J. Nanoparticle Res.*, vol. 14, no. 12, 2012.
- [18]. D. Gopi, M. T. Ansari, E. Shinyjoy, and L. Kavitha. "Synthesis and Spectroscopic Characterization of Magnetic Hydroxyapatite Nanocomposite Using Ultrasonic Irradiation." *Spectrochim. Acta - Part A Mol. Biomol. Spectrosc.*, vol. 87, pp. 245-250, 2012.